ELSEVIER

Applied Ocean Research 26 (2004) 49–60

Applied Ocean Research

www.elsevier.com/locate/apor

Buoy observations of the influence of swell on wind waves in the open ocean

N. Violante-Carvalho[a,*], F.J. Ocampo-Torres[b], I.S. Robinson[a]

[a]*Southampton Oceanography Centre, University of Southampton, European Way, Southampton, SO14 3ZH, UK*
[b]*Departamento de Oceanografia Fisica, CICESE, 22860 Ensenada, Mexico*

Received 5 August 2002; accepted 5 November 2003

Available online 12 October 2004

Abstract

The influence of longer (swell) on shorter, wind sea waves is examined using an extensive database of directional buoy measurements obtained from a heave-pitch-roll buoy moored in deep water in the South Atlantic. This data set is unique for such an investigation due to the ubiquitous presence of a young swell component propagating closely in direction and frequency with the wind sea, as well as a longer, opposing swell. Our results show, within the statistical limits of the regressions obtained from our analysis when compared to measurements in swell free environments, that there is no obvious influence of swell on wind sea growth. For operational purposes in ocean engineering this means that power-laws from fetch limited situations describing the wind sea growth can be applied in more realistic situations in the open sea when swell is present.

Keywords: Wind sea growth; High frequency spectrum; Equilibrium range; Campos Basin; Directional buoy data

1. Introduction

Most of the studies that have tried to address the problem of the growth of wind waves were carried out in laboratory tanks or coastal areas with well known fetches and without swell. The effect of longer waves on the evolution of wind sea is not well investigated in the open ocean where swell is ubiquitous. It is not clear whether or how its presence would change the mechanics of wave growth and to what extent.

The detailed processes that govern the shape and evolution of wind waves are still not completely understood. It is however common knowledge that the growth of waves in deep water is a function of three dynamic processes called source terms, that is, the input of kinetic energy by the wind (S_{in}), energy dissipation due to wave breaking (S_{ds}) (also known as white capping) and nonlinear resonant wave interaction (S_{nl}). It is remarkable that wind waves spanning a variety of wind speed conditions present a similarity in their spectral shape, and although all three dynamic processes play au important role it is believed that the nonlinear interactions are mainly responsible for this 'shape stabilization' process. One of the main features of this universal shape of wave spectra is a high frequency tail decay proportional to a power law in the form $E(f) \propto f^n$ where $E(f)$ is the frequency (or one-dimensional (1D)) spectrum, f is frequency and n is an exponent that determines the rate of decay.

The concept of equilibrium range was fundamental for the description of the evolution of waves under fetch limited conditions. Phillips [1] using dimensional considerations suggested that in the frequency range between 1.5 and 3 times f_p (the peak frequency) due to wave steepness the spectral level is determined mainly by wave breaking. In this region the dynamic processes balance each other, that is $S_{in} + S_{ds} + S_{nl} = 0$ and the input of spectral energy equals the loss of energy yielding a saturation level. Phillips [1] pointed out that the spectral tail that best describes this high frequency band is proportional to the minus fifth power

* Corresponding author. Fax: +44-23-8059-3059.
E-mail address: violante.carvalho@soton.ac.uk (N. Violante-Carvalho).

0141-1187/$ - see front matter © 2004 Elsevier Ltd. All rights reserved.
doi:10.1016/j.apor.2003.11.002

($n=-5$). Later on Phillips [2] reanalyzed the equilibrium range theory and reported that an f^{-4} tail is more appropriate.

The evolution of the wave spectrum is determined by the sum of the dynamical terms S_{in}, S_{ds} and S_{nl} as represented by the energy transfer equation:

$$\frac{\partial E}{\partial t} + \mathbf{C_g} \cdot \nabla E = S_{in} + S_{ds} + S_{nl} \quad (1)$$

where $E=E(f,\theta)$ is the directional spectrum and $\mathbf{C_g}$ is the group velocity. The left hand side of (1) gives the advection of energy for each wave component whereas the right hand side describes the evolution of the spectrum. As a result of the dynamical processes the peak shifts to lower frequencies and broadens as the spectrum becomes more mature.

The study of the interaction of long and short wind waves is also relevant to understanding the processes involved in the modulation of radar backscatter at a shorter wave length scale. Komen et al. [3] solved (1) numerically to study the equilibrium range solution and the dynamics of wave generation and evolution, where they considered for computational reasons the range of frequencies around f_p. Moreover Komen [4] points out that the evolution of short gravity waves can be described from consideration of the source terms and how they interact. For low wind speeds and at an early stage of development very short gravity waves are within the frequency range analyzed by Komen et al. [3] and hence the source terms describe the physical processes involved in their evolution. The imaging of ocean waves by radar, for example the Synthetic Aperture Radar (SAR) imaging mechanism, is based on the interaction of these decimeter waves with longer waves through the process called Bragg resonant scattering. Furthermore most of the models of the tilting modulation transfer function assume a Phillips k^{-4} high wavenumber spectrum though it is not clear what is the best exponent for such models (see for instance Violante-Carvalho et al. [5] and the references therein). Although in the present study we are focusing on longer wind sea and swell waves (with wave lengths longer than 20 m) the discussion might help to clarify how Bragg waves are hydrodynamicaly affected by longer waves.

Energy transfer among wave components due to nonlinear interactions has been considered an important aspect for determining the evolution of the wave directional spectrum since the pioneering JONSWAP experiment in the North Sea. Its influence on the wind generated growth in laboratory experiments has also been determined [6]. Through numerical experiments, the importance of the spectral peaks for swell and wind sea to be closely located within the frequency-direction space, has already been defined [7,8]. It has become clear that the energy transfer considering individual components within the spectra (wind sea and swell) is less than that when considering the combined wind sea and swell in one bimodal spectrum.

More recently Lavrenov and Ocampo-Torres [9], using the exact calculation for the energy transfer due to nonlinear interaction, studied the dependence on the directional spread. Non-zero values for energy transfer were calculated for waves travelling in opposite direction to the wind, specially for wide directional spreading within the spectra. Furthermore, for cases of similar directional spread, the relative nonlinear energy transfer was greater for wider frequency spectra. Within this context, bimodal or trimodal spectra can be viewed as displaying a rather wide directional spreading character. Therefore, this can be an obvious mechanism to influence wind wave growth under the presence of swell.

A number of experiments indicate that wind waves are attenuated in the presence of long waves but the mechanisms which cause the suppression of the wind waves are not clear although several theories have been proposed. Through numerical simulations Masson [8] investigated the effect of nonlinear coupling due to resonant interactions in bimodal spectra in deep water waves. The nonlinear term S_{nl} has been shown to play an important role in the coupling between swell and wind sea causing the swell to grow at the expense of the wind sea in the frequency range just below the peak frequency of the wind sea. The magnitude of the coupling depends on the relative direction of propagation between swell and wind sea, where the coupling is maximum at about 40° [8]. When the direction of propagation of swell moves away from the wind sea direction the nonlinear coupling decreases quickly. That work also considered the influence of swell on wind sea growth in relation to the separation between them in frequency space, where the coupling is not significant for ratios of swell and wind sea peak frequencies ($f_{p_{swell}}/f_{p_{sea}}$) less than about 0.6. A different theory stresses the role of the dissipation term in the suppression of the wind waves. Based on laboratory experiments Phillips and Banner [10] suggested that the reduction in amplitude of wind waves is due to enhanced dissipation S_{ds} caused by modulation of the short waves by the long waves which then increases the surface drift at the crest of the mechanical waves and the premature breaking of the short waves. More recently Chen and Belcher [11] developed a model to explain different results from wave tank experiments. They pointed out the important role of the wind input source term S_{in} and its coupling with the long waves. They supposed that the long wave absorbs momentum from the wind leaving a reduced amount of turbulent flux in the wind which causes a slower development of wind waves.

There is however a lack of evidence from measurements in the open ocean of the influence of swell on wind waves. This is caused partially by the difficulty of isolating wind sea from the swell contaminated spectra. Dobson et al. [12] found no clear influence of opposing swell on wind sea in an experiment carried out in a fetch-limited coastal area. They concluded that the similarity of their results with those of Donelan et al. [13] in a swell free environment, was because of the short fetches involved in both experiments. The first attempt to investigate wind sea growth and dissipation in

a swell dominated area in the open sea was carried out by Hanson and Phillips [14] in the Gulf of Alaska. They computed 236 directional spectra where over a third of the cases were classified as without swell. In addition only 27% of the swell cases (or less than 20% of the total spectra) were aligned with the wind sea direction whereas the great majority of the swell propagated non-aligned with the wind sea. From their results they have found no clear effect of swell on wind sea growth regardless of the direction of swell propagation. They have not mentioned any sort of investigation of the relation between $f_{p_{swell}}/f_{p_{sea}}$ and its possible influence on wind sea growth. In an attempt to address the lack of measurements in the open ocean of the influence of longer waves on shorter waves we analyzed a data set that consists of over 5800 spectra from a heave-pitch-roll buoy deployed in deep water in the South Atlantic.

2. Data and analysis

The Campos Basin, located off the northern part of the state of Rio de Janeiro (Fig. 1), is the most important offshore region in Brazil. In this basin are located tens of oil platforms responsible for around 75% of the oil and gas prospected in the country. This is also a region of strong commercial and tourist activity. Several offshore operations take place daily in the Campos Basin, such as underwater surveys, pipeline laying, platform maintenance, flexible riser inspections and so on. Its operability depends on the most precise possible description of the sea state, in particular the surface waves, to ensure the safety of personnel and to avoid damage to equipment.

The South Atlantic Deep Water Program (PROCAP) was an experiment conducted by the Brazilian Oil Company (PETROBRAS) to study the development of the main meteorological and oceanographic features of the region and their temporal variability. This program consisted of mooring lines with several instruments for both near-surface and deep water measurements of currents, temperature, salinity, dissolved oxygen, pH and pressure. For wind and wave measurements a heave-pitch-roll buoy with meteorological sensors was deployed in the central region of Campos Basin nearly 150 km offshore. From March 1991 to March 1993 the buoy was moored at position 22°31′ *S* and 39°58′ *W* in a depth of 1250 m. The same buoy was redeployed from January 1994 to July 1995 at position 22°38′ *S* and 40°12′ *W* in 1050 m. In this paper we will describe the wave and wind data acquisition and analysis.

2.1. Wind measurements

The buoy was equipped with meteorological instruments for measuring wind, barometric pressure, air temperature, relative humidity and precipitation. Wind speed and direction were measured by two Young propeller-vane anemometers at a height of 3.78 and 4.43 m and the speed value later corrected for the standard height of 10 m using

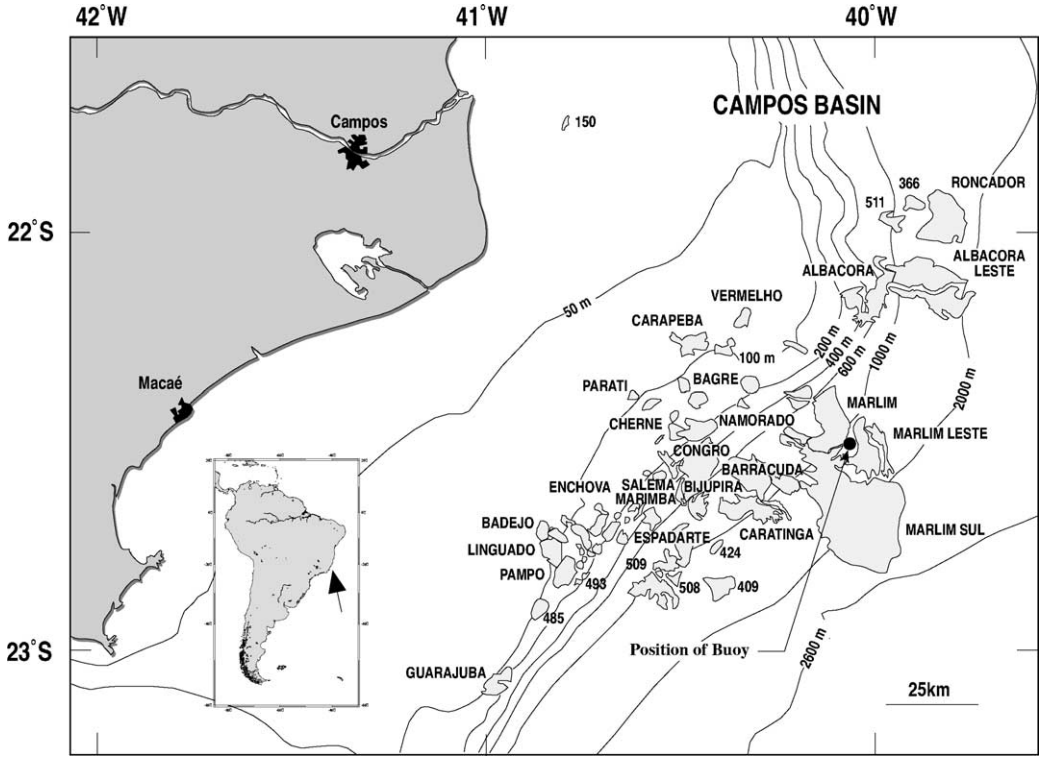

Fig. 1. Position of Campos Basin in the coast off Rio de Janeiro, Brazil and the wave buoy. The shaded areas are the oil fields.

a logarithmic relationship. Each wind measurement is an average of a 10-min record obtained hourly.

Gaps in the wind recorded by the anemometers on the buoy correspond to less than 10% of the total amount of measurements, and were filled with observations obtained on the nearby Enchova Platform located at 22°40′36″ *S* and 40°36′20″ *W*, about 60 km west from the buoy mean position. The wind measurements obtained from the buoy and from the oil platform have a high correlation, both in direction and speed as described in Violante-Carvalho et al. [15], which is attributed to the spatial homogeneity of the wind fields encountered in the region.

2.2. Wave measurements

The heave-pitch-roll buoy, equipped with a Datawell Hippy 120 Sensor, was highly reliable for most of the campaign. However, as the present analysis is interested mainly in the spectral evolution of the wave field over time we consider only the period when there were no, or very small, gaps in the wave record. In this work the wave data comprise the months from February 1992 to January 1993 and from February 1994 to March 1995 totaling 26 months and over 5800 wave spectra.

The buoy recorded three time series, the vertical displacement and two slopes in the east and north directions, at a rate of 1 Hz during 20 min eight times a day every 3 h. Records of 1024 points were segmented in 16 partitions of 64 points yielding 32 degrees of freedom and frequency resolution of 0.015625 Hz using the Welch Method to obtain the spectral estimators (see for example [16]). The classical Fast Fourier Transform (FFT) was applied to all three-time series with a Hanning window and 50% overlap. The directional information was computed using the nonparametric maximum entropy method (MEM) [17].

The high frequency response of the instrument to the sea movement is critical for the analysis performed. The presence of noise generated for example by currents and the mooring system causes a limitation in the buoy frequency range. Furthermore the size of the buoy and its response to the sea displacement together with the accuracy of evaluation of the spectral estimators impose a frequency band from 0.04 to 0.35 Hz [18]. Outside this range the buoy response is questionable and was not considered in the analysis, but for the calculation of the high frequency decay parameter n we have used all the data up to the Nyquist frequency cut-off, that is 0.5 Hz.

2.3. The spectral fitting

A method for spectral fitting and selection of different wave systems of the 1D spectrum was developed and is comprehensively explained in Violante-Carvalho et al. [5] and in this paper we will only give a brief description for completeness. Such a method is of great value for several applications since the wave spectrum is subdivided into a number of different wave systems which can be characterized by a small number of parameters like significant wave height, mean frequency, propagation direction and directional spread among others. Several works have attempted to address the problem of partitioning of the 1D wave spectrum [19–23]. Methods for the partitioning of the directional (or 2D) spectrum have been introduced with the original work by Gerling [24], and later modified by Hasselmann et al. [25]. We however prefer to use only the information yielded directly by the buoy (that is the 1D spectrum from the heave measurements) rather than applying a method for the estimation of the spreading function. We use the MEM rather than the classical Fast Fourier analysis to compute the direction of the wave systems adjusted by the spectral fitting method.

The main assumption in the method by Violante-Carvalho et al. [5] is to consider the 1D spectrum $E(f)$ as the sum of independent wave systems, hence a bimodal spectrum is characterized by a high frequency (E_{hf}) and a low frequency (E_{lf}) system yielding

$$E(f) = E_{\mathrm{hf}} + E_{\mathrm{lf}}. \tag{2}$$

Each wave system E_{hf} and E_{lf} is adjusted using a spectral method based on the JONSWAP spectrum [20]. The JONSWAP spectrum [26] presents a rate of energy decay for the high frequency part which is inversely proportional to frequency to the fifth power ($E(f)^{-5}$). The high frequency tail that best describes the spectral decay is still subject to debate, although in many studies there is a clear evidence that its value lies between -3.5 and -5 [13,27–32]. Liu [33] has reported for experiments in deep water a weak correlation of the high frequency decay at early wave growth stage with the total spectral energy, and for well developed or fully developed waves n seemed to be constant with values between -4 and -3. Young and Verhagen [34] described the gradual decrease in magnitude of n as a function of the effects of finite depth in a shallow lake in Australia. In deep water they found that the exponent is approximately -5 and when the effects of the finite depth become more significant n approaches -3.

To investigate the behaviour of the high frequency tail we employed a spectral form using a variable exponent n in the form $E(f)^{-n}$:

$$E(f) = (2\pi)\alpha g^2 (2\pi f)^{-n} \exp\left[-\frac{5}{4}\left(\frac{f}{f_p}\right)^{-4}\right] \gamma^{\exp\left[\frac{-(f-f_p)^2}{2\sigma^2 f_p^2}\right]}. \tag{3}$$

The exponent n is determined by logarithmic regression of the spectral points beyond 2 times the peak frequency f_p. The parameter α is the high frequency spectral level, γ is the enhancement factor, σ is the spectral width in the peak region and g is the gravitational acceleration. It is worth noting that (3) reduces to the JONSWAP spectrum when n equals -5.

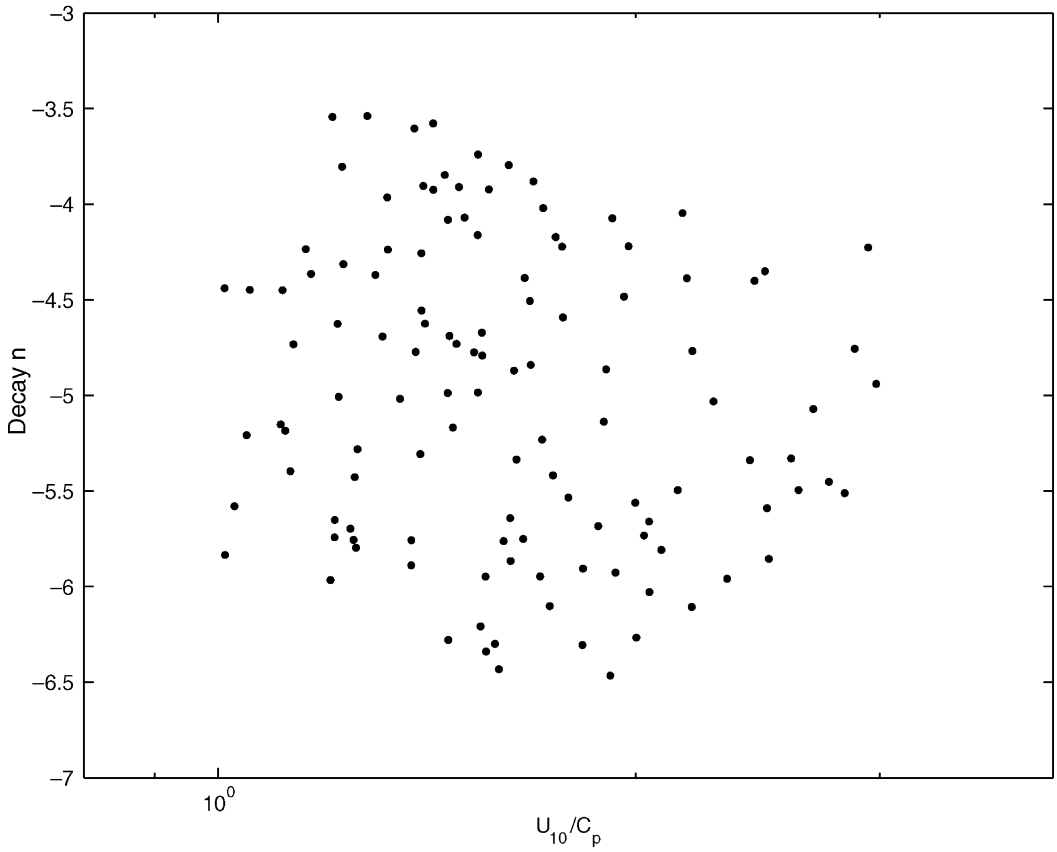

Fig. 2. The exponent n for the cases selected as wind sea as a function of the inverse wave age U_{10}/C_p.

The high frequency decay n obtained from cases selected as wind sea (as defined later in this section) is highly variable although most of its values lie between -4 and -6. Fig. 2 shows values of the exponent n for the cases selected as wind sea against the inverse wave age U_{10}/Cp where Cp is the phase velocity of the wind sea component. There is no clearly predominant decay that supports either $E(f)^{-5}$ or $E(f)^{-4}$, the forms normally encountered in the literature. The best representation of the high frequency tail of the spectrum, or even whether there is a unique value, remains an open question and perhaps a model with a variable exponent n as in (3) is a better approach. However using a constant value of n, either -4 or -5, would allow us to compare our results with previous works where a constant n was employed. We have found no clear dependency of n on other spectral parameters and its value presents a mean equal to -5.01 with a standard deviation equal to 0.78. For this reason we have set the value of n to -5 in (3) and hence we are adopting a JONSWAP model for the spectral fitting.

The first step in the fitting procedure is to select the points of highest spectral ordinate and to check whether they are in fact correlated to different geophysical processes or are a consequence of, for example, sampling variability. Spectra with 32 degrees of freedom and 50% overlap between adjacent segments yielded a satisfactory relation between resolution and variance although further tests are necessary to ensure that a spectral maximum is in fact related to a wave system rather than to fluctuations arising from the spectral estimators (see more discussion about this in Ref. [35]). We adopted three criteria that must all be satisfied for the selection of the spectral peaks:

- each peak must be separated by twice the frequency resolution (0.03 Hz) from adjacent peaks, a rather arbitrary value but which yielded satisfactory results.
- the ratio between the ordinate of the selected peak and of the adjacent one must be less than 15 to eliminate peaks that are below a background noise.
- the two peaks will be accepted if the ordinate of lower limit of the 90 percent confidence interval of the greater peak is higher than the ordinate of the upper limit of the 90 percent confidence interval of the trough between the peaks, which basically means that the valley between the peaks has to be sufficiently low.

The next step in the fitting procedure is to adjust E_{hf}. The values of α and γ are chosen to produce the least-square error between measured and fitted spectra. The adjusted high frequency spectrum is then subtracted from the measured spectrum (2) and the procedure described above

is repeated to adjust the low frequency spectrum in the same way. These procedures outline the fitting of double peaked spectra.

The wave spectra encountered in Campos Basin are quite complex and over a third of the observations fitted using the above criteria present three or more spectral peaks. The fitting procedure for double peaked spectra selects the two most energetic peaks and hence may not select the wind sea system. The main goal of the present analysis is to investigate the influence of swell on the wind sea therefore we must extend the fitting technique. To ensure that the wind sea is always fitted the above procedure was extended to model a third peak, but only if the two initially selected do not correspond to the wind sea. The third peak must also satisfy the three criteria for selection of wave systems. Therefore a trimodal spectrum is represented by

$$E(f) = E_{\text{sea}} + E_{\text{hf}} + E_{\text{lf}} \tag{4}$$

where E_{sea} represents the wind sea system, E_{hf} may represent a young swell and E_{lf} is the swell at lower frequency.

We need reliable criteria to isolate the wind sea from the rest of the spectrum and the wind direction is used as a first condition for the selection. The high frequency peaks that remain within a $\pm 30°$ window of the wind direction measured by the buoy are selected as potential wind sea systems. However in the region of Campos Basin there is a strong presence of a young swell component in propagation directions close to the wind direction and lies in the high frequency part of the spectrum, although not related to the local wind [36]. The equilibrium range theory is then applied as a second criterion for the selection of the wind sea component. Phillips [1] suggested that in the high frequency part of the spectrum (from $1.5f_p$ to $3.0f_p$) the spectrum is proportional to frequency to a power -5 in the form

$$E(f) = \alpha g^2 (2\pi)^{-4} f^{-5}. \tag{5}$$

The high frequency level α is wind dependent and can be used as an indication of the stage of wave growth. This feature is exploited for the selection of the wind sea component of the spectrum. Examination of the data indicates that the wave components above $\alpha = 0.001$ are correlated to the wind energy transfer region and so were classified as wind sea. Fig. 3 presents a typical trimodal spectrum from 1 May 1992 1600 UT with a swell peak at 0.0645 Hz (15.5 s), a young swell at 0.1266 Hz (7.9 s) and wind sea at 0.1887 Hz (5.3 s). The direction that the wind-waves are coming from (not shown on the plot) are, respectively, 145° (SE), 44° (NE) and 33° (NE). Both peaks at higher frequencies lie on a band of active wind input and the wave directional information itself might not be enough for a correct isolation of the wind sea. The figure illustrates a case where the young swell system is just below the equilibrium level for a value of $\alpha = 0.001$. This threshold

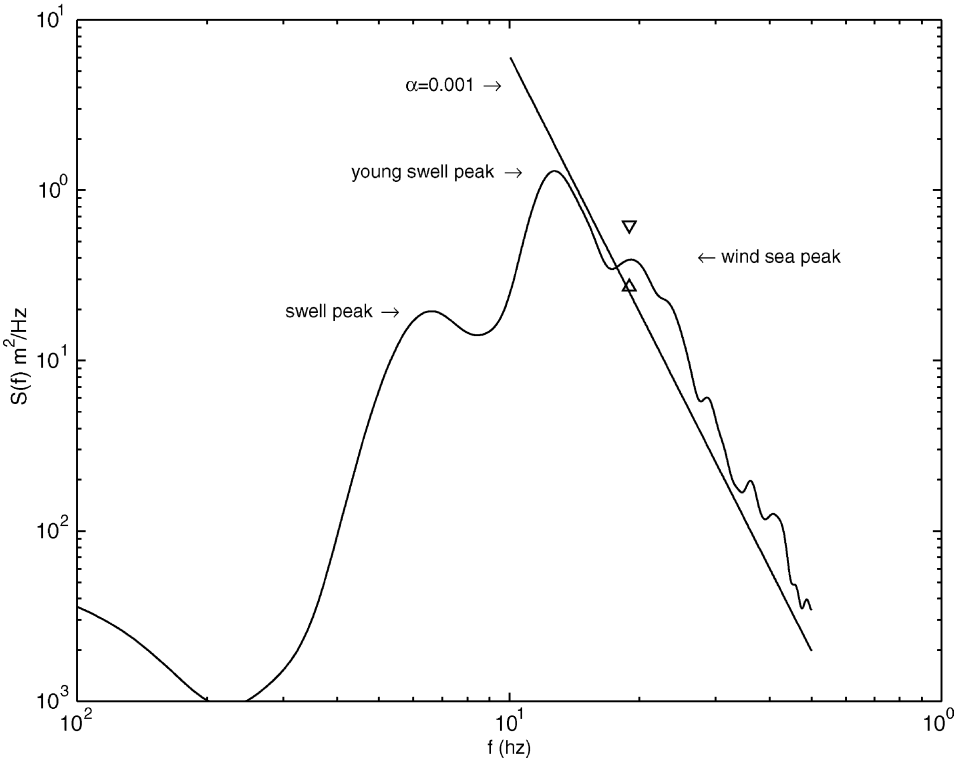

Fig. 3. A trimodal spectrum with the equilibrium range $\alpha g^2 (2\pi)^{-4} f^{-5}$ for $\alpha = 0.001$ included representing the separation between wind sea and young swell. Also appears on the plot the 90% confidence interval represented by the up and down triangles.

value is used in conjunction with the wave directional information for the selection of the wave system generated by the local wind.

3. The influence of swell on wind waves

Violante-Carvalho [36] presented a comprehensive statistical description of the spectral evolution of different wave systems and their relation to the meteorological patterns encountered in Campos Basin. Over one third of the spectra measured in the area present 3 or more peaks which can be explained on the grounds of the prevailing meteorological conditions. In good weather situations the semi-stationary South Atlantic high-pressure center (*H* in Fig. 4) is associated with easterly or northerly winds in the area. The wind sea presents in general peak periods ranging from 3 to 5 s and significant wave heights H_s from 0.25 to 1.25 m. Another wave system is generated nearby associated with the South Atlantic high-pressure center although not related to the local wind in the vicinity of the buoy. Due to the curved form of the isobars around the high-pressure center another wave system is generated with higher directions (20–40° clockwise) than the wind direction measured by the buoy, as can be seen by the arrows indicating the wind direction in Fig. 4. This young swell system, which is always slightly more easterly than the wind sea, has a striking presence in the region with typical peak periods from 5 to 8 s and H_s from 0.5 to 2 m. The young swell is generally associated with longer fetches and more energetic waves than the wind sea and is responsible for severe situations in the area (Parente et al. [37]). In addition lower frequency swell from the southern quadrant with generation areas at higher latitudes is present all the year round in the Campos Basin. Fig. 4 also presents a typical situation of waves generated over 3000 km from the buoy. A cold front represented by black triangles associated with a low-pressure center in the southern extreme of the continent generates a distant swell with peak periods from 8 to 15 s and H_s from 0.5 to 2 m. This is a common situation in Campos Basin, that is, a distant swell propagating in the opposite direction to the wind sea and a young swell propagating close to the wind sea both in direction and frequency. This is an ideal scenario for the investigation of the influence of swell propagation on wind sea growth.

Our analysis was limited to the cases of waves generated by winds whose direction remained relatively stable. The data set was prepared by selecting from 26 months of wind and wave observations the periods in which the wind direction remained within $\pm 20°$ of its mean for at least 4 days. Fig. 5 illustrates one of the nine selected periods of relatively steady wind direction. The selection of steady wind conditions is of fundamental importance for the analysis since varying winds would increase the scatter in the data.

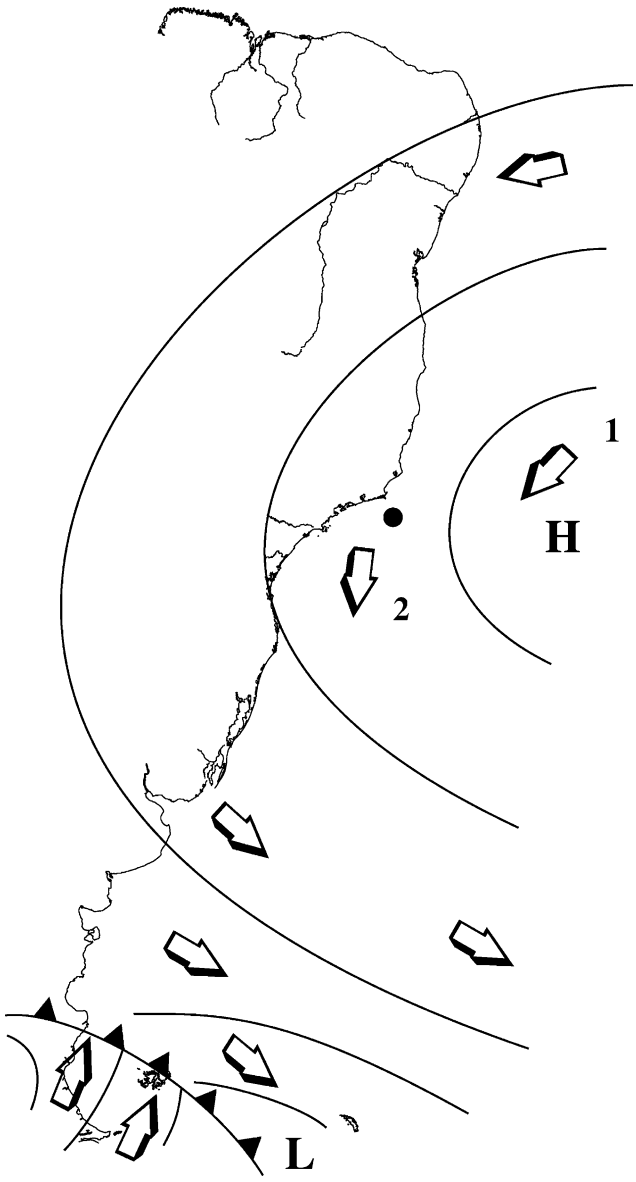

Fig. 4. Schematic representation of the Semi-Stationary South Atlantic High Pressure Center and its influence over the south american continent. The position of the buoy at Campos Basin is represented by the black spot and the direction of the wind responsible for the generation of a young swell and the wind sea is represented respectively by the arrows 1 and 2. At the south extreme of the continent there is a cold front plotted as black triangles associated with the progression of an extratropical cyclone (low pressure center *L*) generating swell from the southern quadrant.

There is a level of uncertainty in our analysis in the band close to the Nyquist frequency associated with waves of small amplitudes. This is firstly due to the high frequency buoy response already pointed out and in second place to the method of spectral partitioning. The partitioning scheme using the 1D spectrum rather than the full directional spectrum may compute an unknown amount of energy from high frequency components of swell propagating in directions other than the local wind. Hence, the spectral fitting method may overestimate the energy variance m_0 due

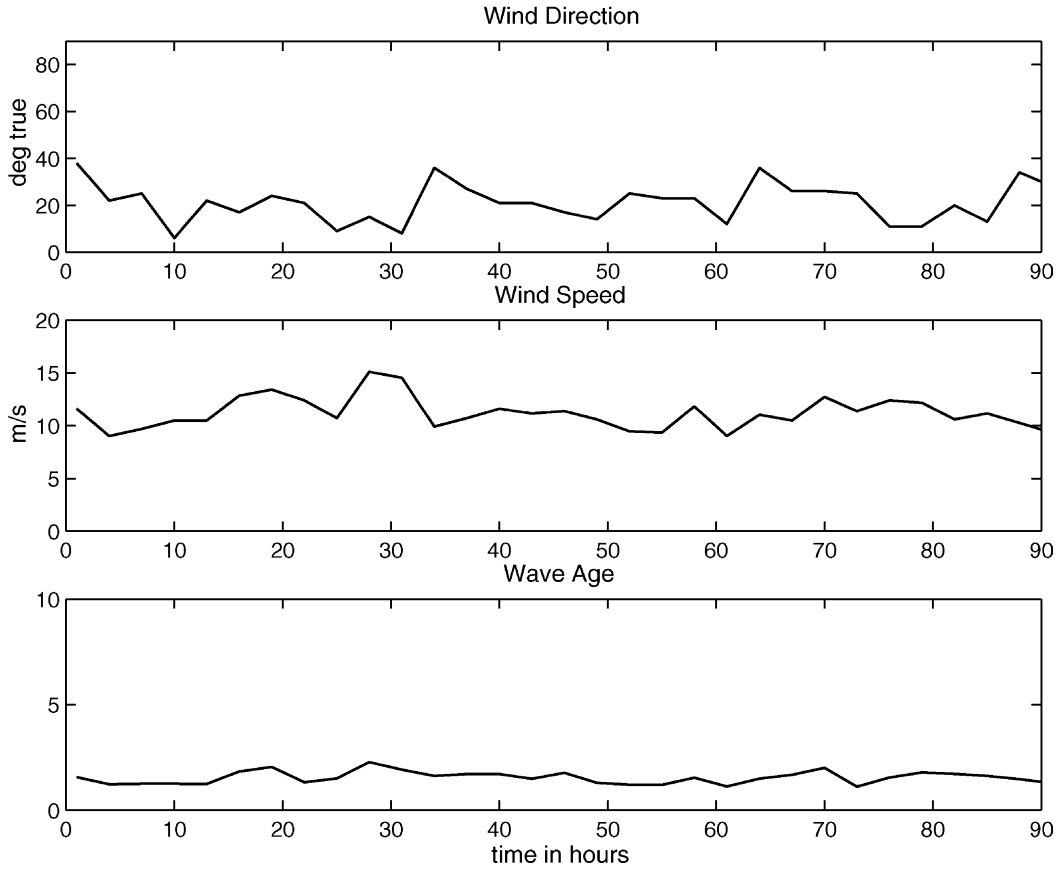

Fig. 5. Respectively from top to bottom time history of wind direction, wind speed and wave age of the wind sea extracted from the model of spectral adjustment observed by the buoy during one of the selected periods of relatively steady wind direction.

to swell contamination of the wind sea spectrum. To mitigate this analysis limitation, and because of the uncertainty of the buoy response to high frequency waves, we eliminated the wave observations where the wind speed U_{10} is less than 7 m/s. Furthermore Donelan et al. [13] proposed that $U_{10}/c_p = 0.83$ corresponds to the value of the spectrum at full development, where the spectral components below this value are classified as swell and above as wind sea. Therefore we dropped the spectra for which $U_{10}/c_p < 0.83$, hence characterized as swell, because of the poorer correlation obtained which yields a total number of 119 ideal cases used in our analysis.

The values of the wind sea high frequency level α isolated by the method of spectral adjustment are plotted in Fig. 6 against the reciprocal wave age U_{10}/c_p. Our results are in remarkable agreement with those obtained in idealized fetch limited conditions, despite the high scatter in the data as observed in similar studies. Due to the process of shape stabilization (see for example [38,39]) the spectral peak shifts to lower frequencies and α decreases due to its response to the wind input of energy. Therefore α has a geophysical meaning and can be used as an indication of the stage of wave development. The evidence that the value of a can be extracted from a multi-modal oceanic spectrum can be useful information for wave forecasting. Once the wind information is available, for example from a scatterometer on board a satellite, the value of α and therefore the stage of wave growth can be used to update wave models.

Table 1 presents the occurrence of directions of swell propagation relative to the wind sea direction. For the trimodal spectral cases swell is considered the closest wave system to the wind sea in frequency space, regardless of whether it is the most energetic system or not. We classified as aligned swell those cases where the direction of propagation of swell is within a $\pm 45°$ window of the wind sea direction and all other cases are considered as non-aligned swell. Moreover Table 1 provides within brackets the number of cases where the ratio between the swell peak frequency and the wind sea peak frequency is less than 0.55 ($f_{p_{\text{swell}}}/f_{p_{\text{sea}}} < 0.55$). Hence considering bimodal spectra there are 13 cases out of 57 where the direction of propagation of the swell peak is aligned with the wind sea and the ratio $f_{p_{\text{swell}}}/f_{p_{\text{sea}}}$ is less than 0.55. Also shown in Table 1 is that from the 37 cases of trimodal spectra there is only one where swell is not aligned with wind sea. This is evidence of the strong presence of a young swell system in Campos Basin, whose peaks are close to the wind sea in terms of direction of propagation and in terms of frequency. Most of the time

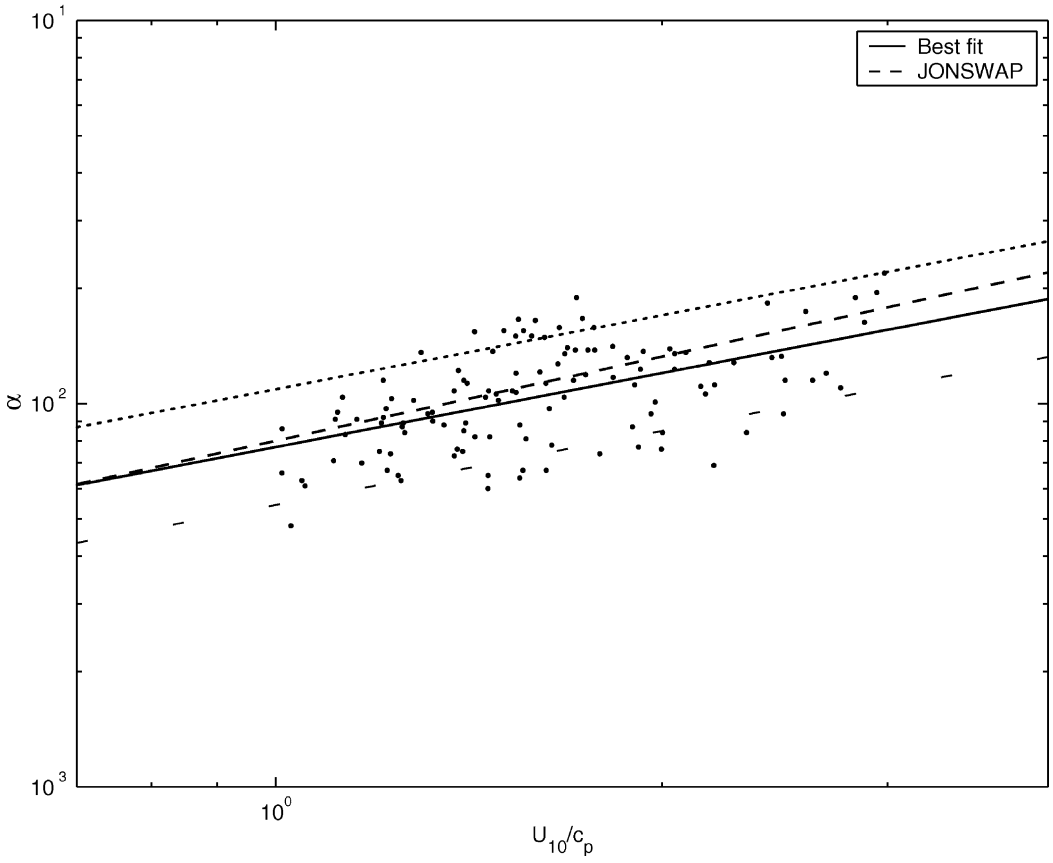

Fig. 6. Values of the 119 cases of high frequency energy level α as a function of the reciprocal wave age U_{10}/c_p. The solid line is the best fit to our data $\alpha = 0.0077(U_{10}/c_p)^{0.64}$ with a correlation coefficient $r = 0.54$, whereas the 90% confidence interval is represented by the dotted lines. The dashed line is from JONSWAP, $\alpha = 0.0080(U_{10}/c_p)^{0.73}$.

the second swell partition of the trimodal spectra propagates from the south quadrant at lower frequencies, usually with generation areas located at higher latitudes [36].

Donelan et al. [40] carried out a detailed field experiment in Lake Saint Clair to explore the wave growth in a fetch-limited swell-free environment. They found a high correlation between the reciprocal wave U_c/c_p and the dimensionless wave energy ε:

$$\varepsilon = 0.0022\left(\frac{U_{10}}{c_p}\right)^{-3.3}. \quad (6)$$

In order to investigate whether the swell dominated environment of Campos Basin produces similar results we searched for the best regression to the data. We present in Fig. 7 the variation of the dimensionless wave energy ε with U_{10}/c_p and the best-fit of the data expressed by

$$\varepsilon = 0.0017\left(\frac{U_{10}}{c_p}\right)^{-3.21} \quad (7)$$

with a correlation $r = -0.82$.

The best fit to the data (7) is in close agreement with Donelan's relationship (6). Hanson and Phillips [14] obtained similar results from their data in the Gulf of Alaska:

$$\varepsilon = 0.0020\left(\frac{U_{10}}{c_p}\right)^{-3.22}. \quad (8)$$

Within the scatter in the data there is no clear evidence of the influence of swell on wind waves, with relations (6)–(8) being statistically identical. However both statistics obtained at open sea data (7) and (8) seem to point to a small reduction on wave energy in the presence of swell in comparison to (6). The relation obtained at Campos Basin (7) seems to indicate a reduction of around 15% on the wind sea energy, whereas in the work by Hanson and Phillips (8) the reduction is less than 5%. It is

Table 1
Occurrence of the direction of swell propagation relative to the wind sea direction in terms of the number of spectral peaks

	Aligned swell	Non-aligned swell	No. obs.
Unimodal	–	–	3
Bimodal	57 [13]	22 [12]	79
Trimodal	36 [1]	1 [0]	37
Total	93 [14]	23 [12]	119

Within brackets are the number of cases where the ratio between the swell peak frequency and the wind sea peak frequency is less than 0.55.

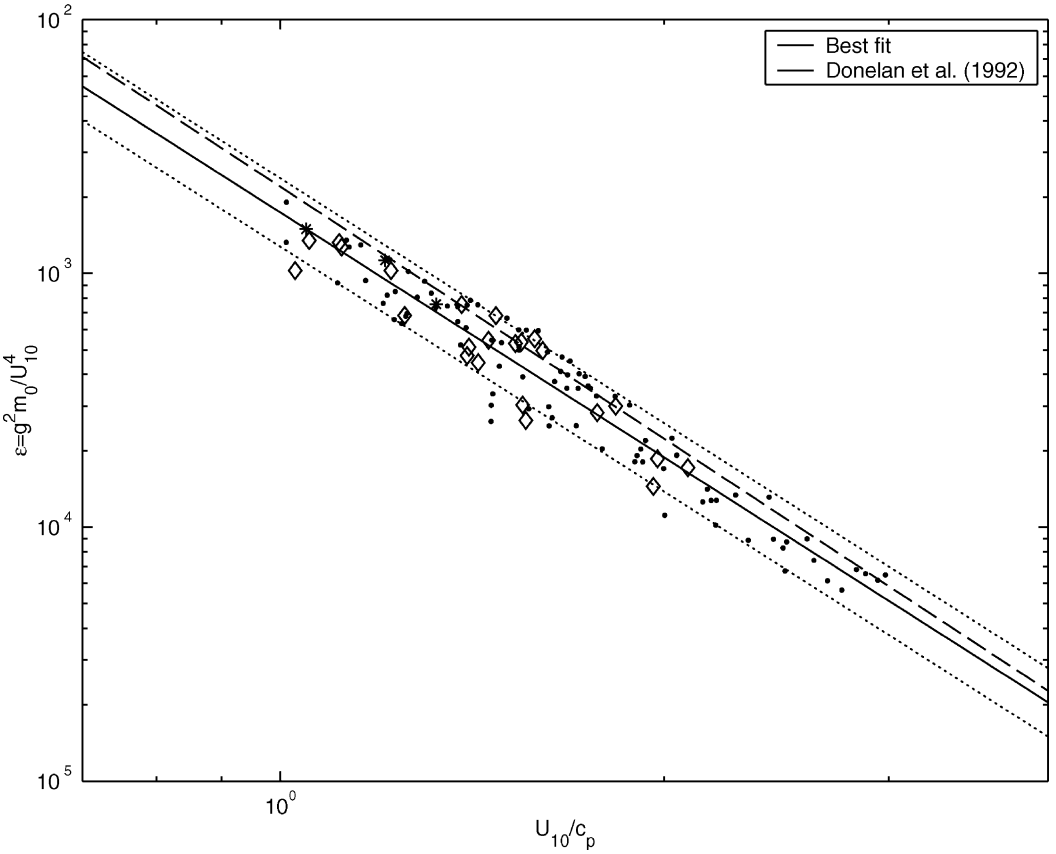

Fig. 7. The dimensionless wind sea wave energy ε as a function of the reciprocal wave age U_{10}/c_p.The solid line is the best fit to the data $\varepsilon=0.0017(U_{10}/c_p)^{-3.21}$ and the dashed line is the power-law regression $\varepsilon=0.0022(U_{10}/c_p)^{-3.3}$ from Donelan et al. [40]. The diamonds are the 23 cases where swell is not aligned with wind sea, the stars are the 3 cases of unimodal spectra whereas the points are the 93 cases where swell is aligned with wind sea (see Table 1). The 90% confidence interval is also shown as the dotted lines.

worth noting that only 18% of spectra measured in the Gulf of Alaska presented swell propagating aligned with wind sea. In contrast over 78% of the spectra used in our analysis present swell propagating close both in frequency and in direction with the wind sea, where one would expect a stronger reduction on wind sea energy due to the presence of longer waves.

There is enough scatter in the plot to extend our analysis to investigate the influence of swell in terms of both direction of propagation and frequency. The best fit to our data considering non-aligned swell and aligned swell (with correlation coefficients $r=-0.89$ and -0.82) is given respectively by

$$\varepsilon = 0.0018\left(\frac{U_{10}}{c_p}\right)^{-3.2} \tag{9}$$

and

$$\varepsilon = 0.0016\left(\frac{U_{10}}{c_p}\right)^{-3.0}. \tag{10}$$

From Fig. 7 it is not clear whether the direction of propagation of swell may affect the wave growth, although looking at (9) and (10) there seems to be a slight decrease in wave energy when swell propagates aligned with wind sea. Considering that most of the swell in Hanson and Phillips [14] is propagating non-aligned with wind sea, that could explain why the relation obtained from their data presents a slightly higher value than ours.

Masson [8] based on simulations concluded that the nonlinear coupling is negligible unless the two peaks are very close in frequency which can make the bimodal structure of the spectrum hard to identify. The data from Campos Basin provides ideal cases for validation of these assumptions. Just to illustrate an example, a wind sea component at 0.189 Hz (5.3 s) and a young swell component at 0.127 Hz (7.9 s) propagating in close directions is a common situation. The spectrum in Fig. 3 illustrates such a situation where the ratio between swell and wind sea peak frequencies is greater than 0.6. The spectral peaks are clearly separated in f space and the method adopted in the present work for the spectral adjustment is able to identify both systems. The regression obtained from the data considering the cases where the ratio $f_{p_{\text{swell}}}/f_{p_{\text{sea}}}$ is less than 0.55 is:

$$\varepsilon = 0.0020\left(\frac{U_{10}}{c_p}\right)^{-3.3} \tag{11}$$

with a correlation coefficient $r = -0.84$. It is worth noting that (11) is closer to the relation obtained in a swell free environment (6), which might be an indication that the separation between the peaks in frequency space is relevant to the suppression of the wind waves. The regression of the 90 data points where $f_{p_{\text{swell}}}/f_{p_{\text{sea}}} \geq 0.55$ (with $r = -0.82$) is

$$\varepsilon = 0.0017\left(\frac{U_{10}}{c_p}\right)^{-3.2} \tag{12}$$

which is the same as relation (7) when we consider the regression of all cases regardless of their direction of propagation or ratio $f_{p_{\text{swell}}}/f_{p_{\text{sea}}}$.

4. Discussion

We have examined in this paper the effect of long waves on the energy of wind sea considering different propagation directions and frequencies of swell. Based on Phillips' equilibrium range theory and applying a spectral method for the adjustment and partitioning we were able to isolate the wind sea from the swell contaminated spectra in a tropical open ocean region in the South Atlantic. From a data set of over 5800 buoy observations we selected cases where the direction of the wind remained stable in direction. The data obtained from the buoy in Campos Basin are unique for the investigation of the influence of swell on wind waves due to the ubiquitous presence of a young swell component propagating aligned with wind sea as well as a longer, opposing swell.

The regression of the values of the high frequency energy level α against the inverse wave age is in very close agreement with similar studies from fetch-limited areas. Such results obtained from multi-modal spectra in the open ocean are remarkable. There is a clear instrument limitation from pitch-roll buoys in the band close to the Nyquist frequency although we have selected only cases of moderate to strong wind speeds to mitigate this problem. Furthermore we have imposed a representation of the high frequency exponential decay in the form $E(f)^{-5}$ although there is no clear indication from our data that a single, constant value should apply. The parameter α is very sensitive to the high frequency band of the spectrum which is a region where one would expect a strong influence of longer waves modulating the shorter, wind sea waves. A possible explanation for such close agreement could be the fact that oceanic waves are longer than those encountered in wave tanks. If the reduction of wind waves as observed in wave tanks is in fact mainly due to nonlinear coupling then longer waves with smaller wave slopes (less nonlinear and hence with weaker nonlinear interactions) would be less sensitive to the presence of swell. However we have found no clear dependency of the wave slope on the energy ratio between sea and swell (not presented here) with the scatter in the data showing no clear trend.

Our measurements show no significant effect of swell on wind sea grow The relation obtained from our observations is similar to the relation proposed by Donelan et al. [40], which is striking due to the differences between the experiments, i.e. a lake without swell and an offshore region where swell is present and is responsible for most of the spectral energy. The relation between wind sea energy and inverse wave age from Campos Basin is statistically identical to the relation obtained in a swell free environment and to another experiment carried out in the open ocean. However there seems to be a small reduction in wave energy in both relations obtained from swell contaminated environments. The observation cases selected in our study when swell is aligned with the wind will exhibit a stronger nonlinear interaction, with the subsequent more active energy transfer. This mechanism will enhance energy distribution so as to reduce the wind sea spectral level. Although a subtle difference is obtained from our results, lower energy level for wind sea under the presence of swell seems to suggest that the nonlinear mechanism is an influencing factor. Further analysis seems to indicate that there is a slight reduction in wave growth when swell propagates close in direction to the wind sea. In addition the regression obtained from our data also seems to point to a minimal reduction on wave growth when swell and wind sea components are close in frequency space, i.e. $f_{p_{\text{swell}}}/f_{p_{\text{sea}}} \geq 0.55$. Nevertheless all the regressions obtained lie within the 90% confidence interval limits which makes it difficult to make firm conclusions from these indications.

Our results are within the statistical limits of the regressions obtained in swell free environments, giving evidence that there is no strong effect of longer waves on wind waves in oceanic regions. If there is in fact any sort of influence of swell on wave growth it seems to us that it is relatively small and considering the present limitations in wave measurement instruments such influence will be masked within the scatter in the data. For practical purposes that means that power-laws obtained from fetch limited situations can be applied in the open sea.

Acknowledgements

We are grateful to PETROBRAS—the Brazilian Oil Company—for making available the buoy data. Violante-Carvalho has been supported by the Brazilian research funding agency CNPq. Ocampo-Torres acknowledges the support from the Mexican Research Council and from the joint programme between the Mexican Academy of Sciences and the Royal Society of London. We would like also to thanks Carlos Guedes Soares for suggestions on an earlier draft.

References

[1] Phillips OM. The equilibrium range in the spectrum of wind-generated waves. J Fluid Mech 1958;4:426–34.

[2] Phillips OM. Spectral and statistical properties, of the equilibrium range in wind-generated gravity waves. J Fluid Mech 1985;156: 505–31.

[3] Komen GJ, Hasselmann S, Hasselmann K. On the existence of a fully developed windsea spectrum. J Phys Oceanogr 1984;14:1271–85.

[4] Komen GJ. The energy balance in short gravity waves. In: Komen GJ, Oost WA, editors. Radar scattering from modulated wind waves. Kluwer; 1988. p. 75–9.

[5] Violante-Carvalho N, Parente CE, Robinson IS, Nunes LMP. On the growth of wind generated waves in a swell dominated region in the South Atlantic. J Offshore Mech Arctic Engng 2002;124:14–21.

[6] Donelan MA. The effect of swell on the growth of wind waves. Johns Hopkins APL Tech Digest 1987;8(1):18–23.

[7] Young IR, Verhagen LA, Banner ML. A note on the bimodal directional spreading of fetch-limited wind waves. J Geophys Res 1995;100(C1):773–8.

[8] Masson D. On the nonlinear coupling between swell and wind waves. J Phys Oceanogr 1993;23:1249–58.

[9] Lavrenov IV, Ocampo-Torres FJ. Angular distribution effect on weakly nonlinear energy transfer in the spectrum of wind waves. Izvestiya, Atmos Oceanic Phys 1999;35(2):254–65.

[10] Phillips OM, Banner ML. Wave breaking in the presence of wind drift and swell. J Fluid Mech 1974;6(Part 4):625–40.

[11] Chen G, Belcher SE. Effects of long waves on wind-generated waves. J Phys Oceanogr 2000;30:2246–56.

[12] Dobson F, Perrie W, Toulany B. On the deep-water fetch laws for wind-generated surface gravity waves. Atmosphere–Ocean 1989; 27(1):210–36.

[13] Donelan MA, Hamilton J, Hui WH. Directional spectra of wind-generated waves. Philos Trans R Soc Lond 1985;A(315):509–62.

[14] Hanson JL, Phillips OM. Wind sea growth and dissipation in the open ocean. J Phys Oceanogr 1999;29:1633–48.

[15] Violante-Carvalho N, Nunes LMP, Tavares Jr. W. Typical conditions and extreme values of wind speed in Campos Basin Technical Report 005/97, Brazilian Oil Company—PETROBRAS 1997.

[16] Marple Jr. SL. Digital spectral analysis. Englewood Cliffs: Prentice-Hall; 1987 p. 492.

[17] Lygre A, Krogstad HE. Maximum entropy estimation of the directional distribution in ocean wave spectra. J Phys Oceanogr 1986;16:2052–60.

[18] Tucker MJ. Interpreting directional data from large pitch-roll-heave buoys. Ocean Engng 1989;16(2):173–92.

[19] Ochi MK, Hubble EN. On six-parameter wave spectra. In Proc 15th Coastal Engng Conf ASCE 1976;321–8.

[20] Guedes Soares C. Representation of double-peaked sea wave spectra. Ocean Engng 1984;11(2):185–207.

[21] McCarthy TJ. Spectral fitting procedures for double peaked wave spectra In Dock and Harbour Engineering Conference, Suratkal, India, 6–9 December 1989.

[22] Guedes Soares C, Nolasco MC. Spectral modeling of sea states with multiple wave systems. J Offshore Mech Arctic Engng 1992;114: 278–84.

[23] Rodriguez G, Guedes Soares C. A criterion for the automatic identification of multimodal sea wave spectra. Appl Ocean Res 1999; 21:329–33.

[24] Gerling T. Partitioning sequences and arrays of directional ocean wave spectra into component wave systems. J Atmos Oceanic Technol 1992;9:444–58.

[25] Hasselmann S, Brüning C, Hasselmann K, Heimbach P. An improved algorithm for the retrieval of ocean wave spectra from Synthetic Aperture Radar image spectra. J Geophys Res 1996;101(C7): 16,615–16,629.

[26] Hasselmann K, Barnett TP, Bouws F, Carlson H, Cartwright DE, Enke K, Ewing JA, Gienapp H, Hasselmann DE, Krusemann P, Meerburg A, Müller P, Olbers DJ, Richter K, Sell W, Walden H. Measurements of wind-wave growth and swell decay during the Joint North Sea Wave Project (JONSWAP). Dtsch Hydrogr Z Suppl 1973; A8(12):95.

[27] Toba Y. Local balance in the air-sea boundary processes, III. On the spectrum of wind waves. J Oceanogr Soc Jpn 1973;29:209–20.

[28] Mitsuyasu H, Tasai F, Suhara T, Mizuno S, Ohkusu M, Honda T, Rikiishi K. Observations of the directional spectrum of ocean waves using a cloverleaf buoy. J Phys Oceanogr 1975;5:750–60.

[29] Banner ML. Equilibrium spectra of wind waves. J Phys Oceanogr 1990;20:984–96.

[30] Prevosto M, Krogstad HE, Barstow SF, Guedes Soares C. Observations of the high-frequency range of the wave spectrum. J Offshore Mech Arctic Engng 1996;118:89–95.

[31] Rodriguez G, Guedes Soares C. Uncertainty in the estimation of the slope of the high frequency tail of wave spectra. Appl Ocean Res 1999;21:207–13.

[32] Young IR. Observations of the spectra of hurricane generated waves. Ocean Engng 1998;25(4–5):261–76.

[33] Liu PC. On the slope of the equilibrium range in the frequency spectrum of wind waves. J Geophys Res 1989;94(C4):5017–23.

[34] Young IR, Verhagen LA. The growth of fetch limited waves in water of finite depth. Part 2. Spectral evolution. Coastal Engng 1996;29: 79–99.

[35] Pierson WJ. Comments on A parametric wave prediction model. J Phys Oceanogr 1977;7:127–37.

[36] Violante-Carvalho, N. Investigation of the wave climate in Campos Basin, Rio de Janeiro—Brazil and its correlation with the meteorological situations—in Portuguese. Master's thesis, Rio de Janeiro University—COPPE/UFRJ; 1998.

[37] Parente CE, Violante-Carvalho N, Lima JAM, Assunção CB. Wave and wind extreme values in good weather situations in Campos Basin, off Rio de Janeiro In Proceedings of the 20th International Conference on Offshore Mechanics and Artic Engineering—OMAEO1 2001.

[38] Komen GJ, Cavaleri L, Donelan MA, Hasselmann K, Hasselmann S, Janssen PAEM. Dynamics and Modelling of Ocean Waves. Great Britain: Cambridge University Press; 1994 p. 532.

[39] Young IR. Wind generated ocean waves. Amsterdam: Elsevier; 1999 p. 288.

[40] Donelan MA, Skafel M, Graber H, Liu P, Schwab D. On the growth rate of wind-generated waves. Atmosphere–Ocean 1992;30(3): 457–78.